ACS OMEGA

http://pubs.acs.org/journal/acsodf

Article

Novel Copper Oxide-Integrated Carbon Paste Tirofiban Voltammetric Sensor

Ameena M. Al-bonayan, Jalal T. Althakafy, Ali Q. Alorabi, Nasser A. Alamrani, Enas H. Aljuhani, Omaymah Alaysuy, Salhah D. Al-Qahtani, and Nashwa M. El-Metwaly*

Cite This: *ACS Omega* 2023, 8, 5042−5049

Read Online

ACCESS | Metrics & More | Article Recommendations | Supporting Information

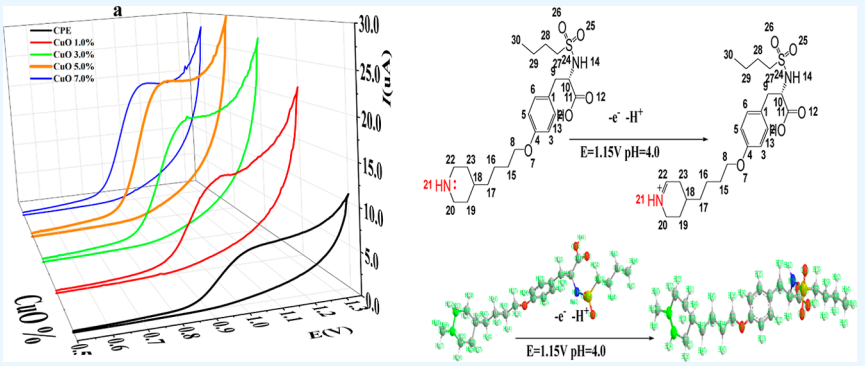

ABSTRACT: The present study introduced the construction and electroanalytical characterization of novel tirofiban (TIR) carbon paste voltammetric sensors integrated with copper oxide nanoparticles. The copper oxide nanostructure remarkably enhanced the oxidation of TIR molecules on the electrode surface with an irreversible anodic oxidation peak at about 1.18 V. The peak current values of the recorded differential pulse voltammograms were correlated to the TIR concentrations within a defined linear range from 0.060 to 7.41 μg mL^{-1} with an LOD value of 20.7 ng mL^{-1}. Based on the electrochemical behavior of TIR at different scan rates and with the aid of the molecular orbital calculations performed on the TIR molecule, the electro-oxidation reaction was postulated to undergo through the oxidation of the five-membered-ring nitrogen atom with the transfer of one electron and one proton. Based on the reported selectivity and sensitivity of the proposed method, TIR was successfully determined in Aggrastat intravenous infusion and biological samples with mean average recoveries agreeable with the UV spectrophotometric method.

1. INTRODUCTION

Due to vascular injury, blood platelets were activated by local agonists, such as thrombin, collagen, and epinephrine, which resulted in adhesion and aggregation of the platelets. This is a consequence of a conformational change in certain glycoprotein receptors (GP IIb/IIIa) on the surface of the platelet, allowing the binding of fibrinogen and subsequent cross-linking of the platelets.[1] Through binding with several glycoprotein IIb/IIIa receptors, fibrinogen simultaneously activates cross-linking of platelets and promotes their accumulation and finally thrombus formation.[2] Therefore, compounds that inhibit this binding are capable to eliminate thrombus formation and reduce the incidence of ischemic complications after coronary restenosis. Tirofiban (TIR, *N*-(*n*-butanesulfonyl)-*O*-(4-(4-piperidinyl)-butyl)-(*S*)-tyrosine) is a potent reversible, fast-acting, and specific peptidomimetic (nonpeptide) glycoprotein receptor antagonist through the inhabitation of the fibrinogen-dependent platelet aggregation and prolongs bleeding times in patients with acute coronary syndromes. TIR is essential for patients suffering from vaso-occlusive disorders such as unstable angina pectoris and myocardial infarction.[1,3,4] Its mechanism of action is based on the competitive inhibition of the aggregation of the activated platelets through binding with the membrane-bound glycoprotein complex (GPIIb/IIIa), preventing the binding of fibrinogen, von Willebrand factor (vWF), and other adhesive ligands.[5] Recently, TIR treatment in acute ischemic stroke has been made more popular by endovascular therapy (AIS).[1,6] TIR attains more than 90% inhibition by the end of the 30 min infusion after its administration. TIR also has been appeared to be effective in reducing ischemic complications associated with the percutaneous coronary intervention.[5]

TIR is unofficial in pharmacopeia; moreover, only few chromatographic and spectrometric approaches were reported

Received: December 6, 2022
Accepted: January 9, 2023
Published: January 24, 2023

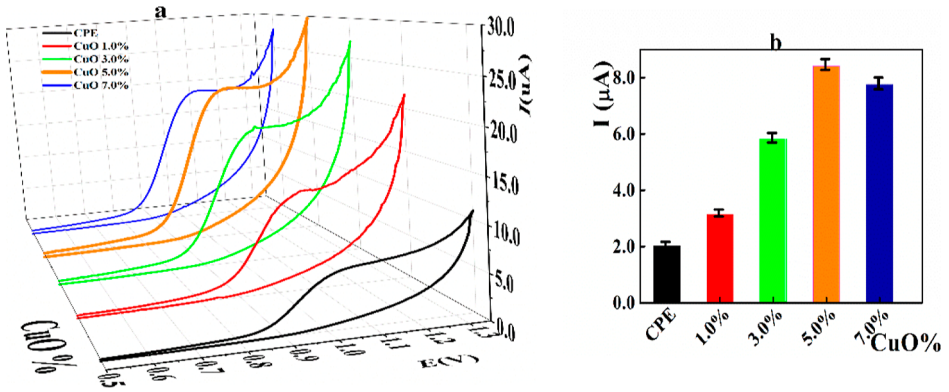

Figure 1. (a) Voltammetric behavior of TIR at carbon paste sensors incorporated with different ratios of CuONPs at pH 4.0 and (b) peak heights at different ratios of CuONPs. Scan rate 60 mV s^{-1}.

to monitor TIR residues in bulk, dosage forms, and biological fluids. Chromatographic methods based on HPLC-UV,[7] RP-HPLC,[8−11] and liquid chromatographic-mass spectrometry (LC−MS)[4,12,13] were found in the literature. The chiral separation chromatographic method utilizing hydroxypropyl-γ-cyclodextrin (HP-γ-CD) as the chiral mobile phase was evaluated for selective separation of TIR enantiomers in samples with UV detection at 226 nm.[14] UV and spectrofluorimetric methods were adopted for the determination of TIR in pharmaceutical formulations with acceptable sensitivity.[15,16] A radioimmunoassay approach was reported for monitoring of TIR in plasma; however, it is not commercially available.[17]

Even though the aforementioned chromatographic approaches sustain high sensitivity, however, they are time-consuming with multiple sample pretreatment steps utilizing expensive operational instruments and not appropriate for routine analysis of large samples. TIR is commonly prescribed to the patient; therefore, a simple, precise, sensitive, and reliable analytical protocol for TIR quantification in different samples is welcomed. Electroanalytical techniques based on tailormade electrochemical sensors have been proven to be an excellent choice for monitoring pharmaceutical and bioactive compounds in different medicinal formulations and biological samples.[18−29] With the advantages of acceptable sensitivity, relatively short analysis time, and simple instrumentation equipment, the electroanalytical approaches can contribute to the analysis of pharmaceuticals in quality control laboratories as an alternative or the committee with other spectrometric and chromatographic techniques. Moreover, exploring the electrochemical behavior of a drug molecule may be useful for explanation of its vivo redox processes, metabolic fate, or pharmacological activity.

While developing a new voltammetric approach, trials were carried out to integrate the working electrodes with various metallic nanostructures aiming at the enhancement of the sensor performance, which in turn improves the sensitivity and selectivity of the method. Based on their electrocatalytic activity and ability to catalyze the electrode process via a noticeable lowering of overpotential, metal oxide nanostructures act as one of the most common electrode modifiers.[30−43] To the best that we can tell, no electroanalytical approach was reported for assaying of TIR, and the electrochemical analysis of TIR at carbon paste electrodes integrated with the copper oxide nanoparticles (CuONPs/CPE) is presented for the first time. It comprises investigations of the influence of the electrode modifier, pH of the supporting electrolyte, and variation of scan rate, and other measuring parameters were evaluated.

2. EXPERIMENTAL SECTION

2.1. Reference Drug and Reagents. The authentic TIR sample ($C_{22}H_{36}N_2O_5S{\cdot}HCl$, 495.08 g mol^{-1}, assigned to contain 101.11%) was provided by Gland Chemical Private LTD (Egypt). The drug stock solution was freshly prepared by dissolving the required amount of the reference TIR standard sample in bi-distilled water and kept in a regenerator at 4 °C. Carbon paste matrices were prepared using graphite powder (Aldrich) and paraffin oil (PO, Merk). Copper oxide nanoparticles (Alfa Aesar, 30−50 nm) were incorporated in the paste matrix as an electrode modifier. BR buffer (4.0×10^{-2} mol L^{-1}) was selected as the supporting electrolyte.

2.2. Electrodes and Measuring Apparatus. Carbon pastes were prepared by intimate mixing of 200 mg of graphite powder with 80 μL of PO. The homogeneous paste was packed into the electrode body as described in detail elsewhere.[44] To obtain a new working electrode surface, the piston screw was pushed and the surface was polished with wet filter paper. The copper oxide nanoparticle-integrated pastes were fabricated in the same manner by replacing 10 mg of the graphite powder with the CuONPs. Voltammetric analyzer station 797 VA (Metrohm, Switzerland) was used for voltammetric measurements accompanied by a three-electrode measuring cell composed of the working carbon paste electrodes (CPE), Ag/AgCl double junction reference electrode, and platinum wire as an auxiliary electrode.

2.3. Optimized Measuring Parameters. Ascending increments of the TIR standard solution were added to the measuring cell containing 15 mL of BR buffer at pH 4. Differential pulse voltammograms were recorded under the following electroanalytical parameters: pulse height 50 mV; pulse width 100 ms; pulse duration 40 ms; and scan rate 60 mV s^{-1}. The recorded peak heights were plotted against the corresponding TIR concentration in the microgram range.

2.4. Analysis of Samples. Aggrastat intravenous infusion samples manufactured by Algorithm (sterile solution in water for injection contains 5.618 mg of TIR, sodium chloride, sodium citrate, and citric acid) were obtained from local drug stores. The pharmaceutical sample solutions were assayed after the proper dilution according to the presented voltammetric approach in accordance to the UV method.[15]

https://doi.org/10.1021/acsomega.2c07790
ACS Omega 2023, 8, 5042−5049

Table 1. Comparison of the Active Surface Area and Redox Characteristic Peak of Different Studied Electrodes

sensor	E_{pa} (V)	E_{pc} (V)	ΔE (V)	I_{pa} (A)	I_{pc} (A)	I_{pa}/I_{pc} (A)	active area (cm^2)
CPE	0.412	0.331	0.081	1.01×10^{-5}	-0.74×10^{-5}	−1.3648	0.025
CuO 1.0%	0.408	0.329	0.079	1.53×10^{-5}	-0.96×10^{-5}	−1.5938	0.0391
CuO 3.0%	0.405	0.333	0.072	1.81×10^{-5}	-1.5×10^{-5}	−1.2067	0.045
CuO 5.0%	0.402	0.327	0.075	2.65×10^{-5}	-1.8×10^{-5}	−1.4722	0.115
CuO 7.0%	0.405	0.333	0.072	2.18×10^{-5}	-1.6×10^{-5}	−1.3625	0.093

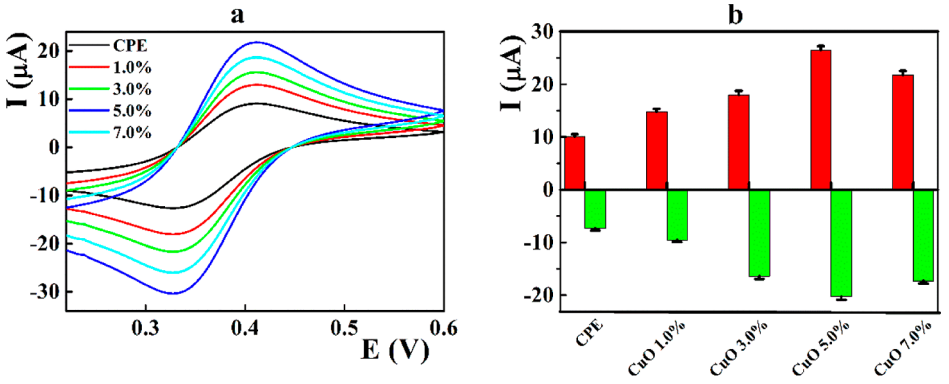

Figure 2. (a) Cyclic voltammograms recorded in FCN solution at the carbon paste electrode modified with different CuONPs ratios and (b) peak current of cathodic and anodic peaks recorded at different CuONPs ratios.

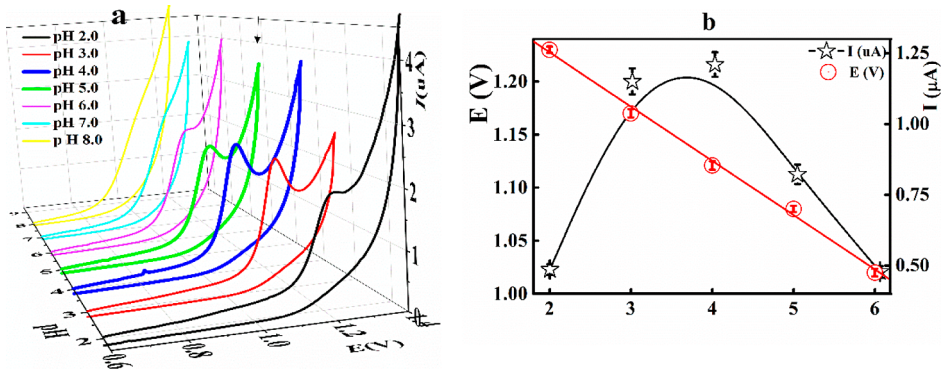

Figure 3. (a) Voltammetric behavior of TIR molecules (5.0 μg mL^{-1}) at CuONPs/CPE recorded at different pH values and (b) peak potentials and currents against pH values.

Biological plasma samples were strengthened with suitable aliquots of TIR stock solution, treated with acetonitrile, and centrifuged for 10 min at 4000 rpm to remove the residual protein, and the TIR contents in the clear supernatant were analyzed voltammetrically compared with the UV method. Samples of urine were laced with standard TIR solution and treated with methanol to remove protein, and the TIR content was assayed as usual.

2.5. Acidic, Basic, and Oxidative Degradation of TIR. TIR was subjected to the degradation under the hydrolysis conditions (either acidic or alkaline) or oxidative degradation as prescribed by ICH guidelines. Simply, 25 mg of the TIR authentic sample was separately dissolved in 25 mL of 1.0 mol L^{-1} NaOH or HCl. The mixtures were refluxed at 75 °C for 30 min,[16] and the progress of the degradation process was monitored by withdrawing samples and following the absorbance at 225 nm. For the oxidative degradation, the TIR sample was dissolved in 25 mL of 3.0% H_2O_2 solution and kept at room temperature for 12 h. After evaporation till dryness, the residue was dissolved in an appropriate volume of water and assayed voltammetrically under the optimized conditions.

3. RESULTS AND DISCUSSION

3.1. Oxidation of TIR at the CuONPs/CPE. Due to slow and slothful electron transfer on the unmodified carbon paste electrode surface, TIR molecules showed a broad irreversible anodic oxidation peak at 1.02 V with low peak current (Figure 1a). Upon incorporation of the copper oxide nanostructures within the electrode matrix, a noticeable enhancement of the peak current was observed. As illustrated in Figure 1b, the peak height was gradually improved upon increasing the CuONP content to reach its maximum value (more than fourfold) at 5% CuONPs. Higher modifier content did not significantly improve the peak performance, which may be explained on the basis of the change in the physical properties and homogeneity of the carbon paste matrix at higher CuONP contents and addition of extra pasting liquid.

For further explanation of the electrocatalytic effect of CuONPs on the electrode performance, cyclic voltammograms were recorded in ferricyanide (FCN) solution as a redox probe (Table 1 and Figure 2). Among different tested CuONP contents, high and well-defined redox peaks were monitored at the 5.0% CuO modified electrode. Compared with the curves

https://doi.org/10.1021/acsomega.2c07790
ACS Omega 2023, 8, 5042−5049

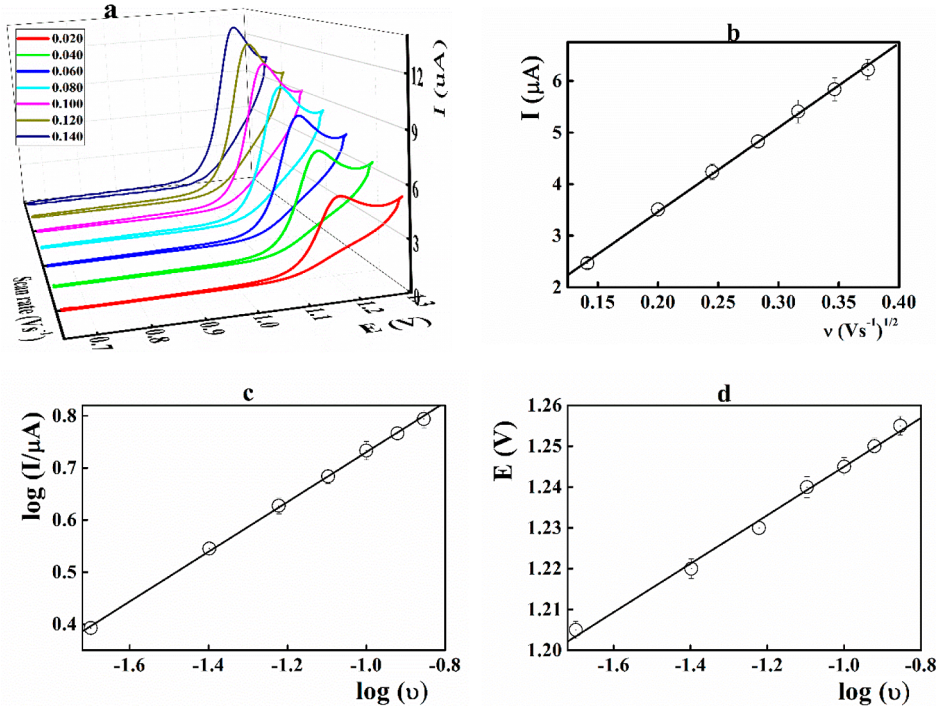

Figure 4. Cyclic voltammograms for 5.0 μmL^{-1} TIR at CuONPs/CPE recorded (a) at different sweep rates, (b) peak current against the square root of the scan rate, (c) logarithmic value of the peak current against logarithmic value of the scan rate, and (d) peak potential against the logarithmic value of the scan rate.

recorded at CPE (10.1 μA, ΔE = 81 mV), CuO 1.0% (15.3 μA, ΔE = 79 mV), and CuO 3% (18.3 μA, ΔE = 72 mV), the 5.0% had higher current values and smaller potential separations. The obtainable results verified that modification with copper oxide nanostructures can improve the electron transport on the electrode surface and enhance the overall electrochemical performance.

Cyclic voltammograms were recorded at different scan rates (from 0.02 to 0.200 V s^{-1}) applying 5.0 × 10^{-3} mol L^{-1} $[Fe(CN)_6]^{3-/4-}$ as a redox probe to evaluate the electroactive surface area of fabricated sensors. The peak current density showed a linear dependence with the square root values of scan rate, indicating the diffusion-controlled process followed in the $[Fe\ (CN)_6]^{3-/4-}$ system on the electrode surface. The electroactive surface area of each electrode can be estimated following the Randles−Sevik equation[45] and was improved from 0.025 cm^2 for the bare electrode to 0.115 for the 5.0% CuO-modified electrode.

3.2. Effect of pH. The impact of the working pH value on the performance of the TIR oxidation peak was evaluated over a wide pH range from 2.0 to 8.0 (Figure 3). About threefold amplification of the peak current was recorded at pH 3.0 compared with that monitored at pH 2.0. Sharp and well-defined oxidation peaks were monitored at pH 3−4 (compatible with the monograph pK_a value of TIR[2]), while at evaluated pH values, the oxidation peak performance decreased and completely disappeared at pH 7.0 (Figure 3a).

The oxidation peak potential was shifted toward the negative direction at higher pH values, indicating the rules of protons in the electrochemical oxidation of TIR molecule on the electrode surface.[46] Constructing the oxidation peak potential (E_V) against the pH value of the supporting electrolyte reveals a linear relationship with near Nernstian slope value ($E_{(V)}$ = −0.051 ± 0.001 [pH] + 1.3282 and r = −0.9980), indicating the equality of the number of protons and electrons that involved in the electro-oxidation of TIR molecules on the electrode surface (Figure 3b).

3.3. Effect of Scan Rate. Evaluating cyclic voltammograms recorded at different scan rates offers valuable information about the electrochemical oxidation mechanism on the electrode surface and the number of electrons that participate in the electrode reaction.[46] Herein, the electrochemical behavior of TIR molecules on the CuONPs/CPE surface was evaluated at different scan rates ranging from 0.020 to 0.140 V s^{-1} at the appropriate pH value (Figure 4a). The peak current was enhanced and the peak position was shifted to the positive direction by increasing the scan rate, indicating the irreversibility of the electrode reaction. Moreover, a linear relationship with a high correlation coefficient (r = 0.9993) was constructed between the peak current and the square root value of the applied scan rate sustaining the irreversibility of the electro-oxidation of the TIR molecule on the electrode surface (Figure 4b). To evaluate the electrode reaction mechanism, the logarithmic values of the peak current were plotted against the corresponding logarithmic value of the scan rate (Figure 4c). Linear relationship (log ($I_{\mu A}$) = 0.4773 log υ (V s^{-1}) + 1.2050; r = 0.9996) with an estimated slope value (0.4773) was close to the theoretically expected value for diffusion-controlled reaction.[47,48]

The number of electrons that participate in the electrode reaction can be calculated by constructing the linear relation between the peak potential versus the logarithmic value of the scan rate ($E_{(V)}$ = 0.0597 ± 0.002 log υ (V s^{-1}) + 1.3048; r = 0.9974, Figure 4d). Based on the Laviron equation for an irreversible process,[49] the number of electrons that participate in the electrode reaction, electron transfer coefficient (α), the standard heterogeneous rate constant of the reaction (k), and the formal redox potential (E^0) can be estimated as follows

https://doi.org/10.1021/acsomega.2c07790
ACS Omega 2023, 8, 5042−5049

Scheme 1. Electrochemical Oxidation Mechanism of TIR at the CuONPs/CPE

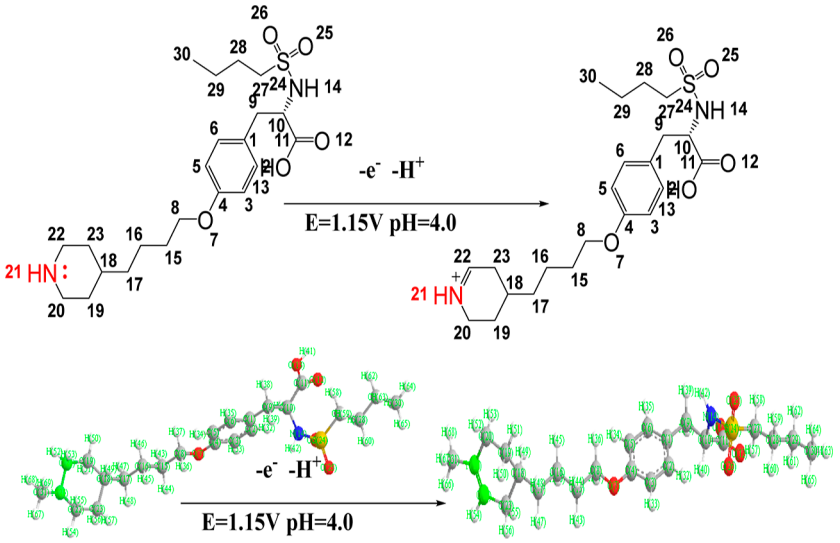

$$Ep = E^0 + \left(\frac{2.303RT}{\propto nF}\right)\log\left(\frac{RTk^0}{\propto nF}\right) + \frac{2.303RT}{\propto nF}log$$

$\upsilon$the value of "α" can be easily estimated from the potential versus Log (υ/V s^{-1}) relation in which the slope was 0.0597, where T = 299 K, R = 8.314 J K^{-1} mol^{-1}, and F = 96485 C mol^{-1}. The estimated value of α was 0.939. The value of formal redox potential (E^0) can be estimated from the intercept of the peak potential against the scan rate (υ/V s^{-1}) curve by extrapolating to the vertical axis at υ value 0. Next, the value of k^0 can be driven from the intercept of Figure 4d.[49,50] The intercept for EP/V versus log (υ/V s^{-1}) plot was 0.982, E^0 was obtained to be 0.965, the k^0 was found to be 675 s^{-1}.

To the best of our knowledge, there is no previous investigation for the electro-oxidation mechanism of the TIR molecule. With the aid of molecular orbital calculations performed on TIR molecules,[51] the most probable mechanism may occur with transfer of one electron through the oxidation of the five-membered-ring nitrogen atom (N21) with the liberation of one proton and the formation of the double bond with the adjacent carbon atom (Scheme 1 and Table S1). Figure S2 presents the chemical structures of TIR at the lowest energy conformations HOMO displays electron density spread in definite regions of the molecule, the likely region of the compound's oxidation (Table S1). In this meaning, the amine moiety of each compound is where the HOMO orbital is distributed (Figure S2). This indicates that this (N21) amine group is probable to be a distributed electrically active site that has a high electro-oxidative potential. This indicates that the nitrogen atom (N21) is probable to be a distributed electrically active site that has a high electro-oxidative potential.

3.4. Method Validation. By performing differential pulse voltammograms under the optimum measuring conditions described above, the performance of the newly fabricated copper oxide nanoparticle-integrated carbon paste electrodes were evaluated for voltammetric determination of TIR. Differential pulse voltammograms were recorded for each TIR increment, and the estimated peak heights (based on base line correction) were plotted against the corresponding TIR concentration in the μg range (Figure 5 and Table 2). The constructed calibration graphs were linear (r = 0.9995) within the TIR concentration ranging from 0.060 to 7.410 μg mL^{-1}.

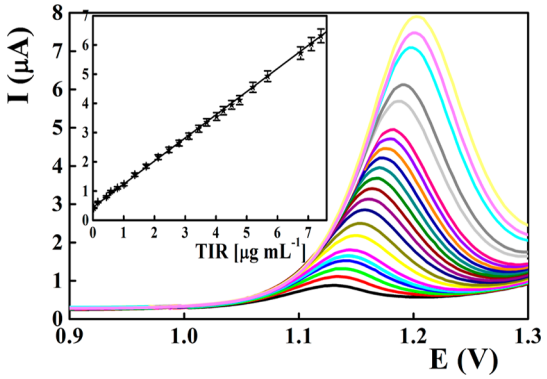

Figure 5. Differential pulse voltammetric definition of TIR at copper oxide nanoparticle-based carbon paste sensors; the operational pH value was 4.0 with a scan rate of 60 mV s^{-1}.

Table 2. Performance Characteristics of the TIR Copper Oxide Nanoparticle-Integrated Carbon Paste Electrode

parameters	value
pH	4.0
peak potential (V)	1.18
linear rang (μg mL^{-1})	0.06−7.41
intercept (μA cm^{-2})	0.4642
slope (μA mL^{-1}/μg)	0.7994
SD of intercept (μA cm^{-2})	0.005
SD of slope (μA mL^{-1}/μg)	0.004
multiple R	0.9995
R square	0.9994
standard Error	0.042
RSD	1.412
LOD (μg mL^{-1})	0.0207
LOQ	0.0629
operational lifetime (month)	4
peak current repeatability of the (RSD %)[a]	1.31
peak current reproducibility (RSD %)[a]	0.94
repeatability of the peak potential (RSD %)[a]	1.25

[a]Obtained from an average of five experiments.

https://doi.org/10.1021/acsomega.2c07790
ACS Omega 2023, 8, 5042−5049

The estimated limit of detection (LOD) and limit of quantification (LOQ) values were 0.0207 and 0.0629 μg mL^{-1}, respectively.[19,20]

The reproducibility of the measurement was evaluated via recording of the successive differential pulse voltammograms for 4.0 μg mL^{-1} TIR solution on the same electrode surface renewed by polishing with a wet filter paper after different intervals within the same day. The relative standard deviation of the recorded peak current was 0.94%. Based on the electrode modification protocol through bulk modification of the electrode matrix with CuONPs, the fabricated sensors showed a prolonged operational lifetime of about 2 months during which the sensor performance remained constant (90.0 ± 2.0%).

3.5. Interference. Different additives and excipients are usually present in the dosage formulations which may result in false information about the active ingredient. For a newly developed method, the influence of different interfering species must be considered. According to the producers, the iso-osmotic intravenous injection was assigned to contain TIR hydrochloride as an active ingredient in the presence of sodium chloride, sodium citrate, and citric acid as additives. Performing differential pulse voltammograms for 4.0 μg mL^{-1} TIR in the presence of the aforementioned additives revealed no significant interference of these interferents. TIR was reported to form metallic complexes $[M(TIR)_2]^{2+}$, through the carboxylic group with some metal cations.[2] These complexes showed improved stability due to the formation of hydrogen bonding and the formation of stacking interactions involving the phenyl ring of the tyrosine residue. Therefore, it is expected that the presence of certain metallic species may lead to negative interference.

Negligible alteration in pharmaceutical formulations can lead to significant changes in the safety of the medicinal product.[52] Continuous development of suitable, sensitive, and reliable analytical methodologies is required to ensure the effectiveness and quality of the medicines. To ensure safety, the proposed approaches should be stability-indicating and enable the identification and determination of levels of the parent compound in the presence of other impurities or degradation products in commercial formulations. Herein, the base hydrolysis of TIR performed at 75 °C for 30 min revealed degradation of 40% of the parent compound, while the corresponding acidic degradation resulted in 32% degradation. Oxidative degradation with H_2O_2 caused 50% degradation which comes in agreement with previously reported values.[11] None of the degradation products exhibited electrochemical activity or voltammetric peaks near that recorded for TIR; therefore, the presented analysis protocol can be considered as the stability-indicating analysis protocol.

3.6. Sample Analysis. The proposed copper oxide nanoparticle-integrated sensors exhibited improved sensitivity and selectivity toward TIR; therefore, they can be utilized as an efficient tool for voltammetric quantification of TIR in pharmaceutical formulation and biological fluids. Samples were spiked with defined TIR concentrations and assayed by measuring the absorbance at 225 nm and voltammetrically following the presented analytical protocol. The low relative standard deviations with acceptable mean recoveries encourage the applicability of the proposed analysis protocol for assaying of TIR (Tables 3 and 4). Based on the Student's t and F tests, no statistical difference between the developed voltammetric approach methods and the UV method was detected regarding accuracy and precision, so the presented sensor can contribute to the monitoring of TIR in quality control laboratories as an alternative or complementary approach.

Table 3. Accurateness of the Estimated Differential Pulse Voltammetric Technique for Determination of TIR in the Pharmaceutical Form

aggrastat	added (μg mL^{-1})	found (μg mL^{-1})	bias %[b]	recovery (%)	UV[15]
	0.58	0.58	0.02	99.98	100.12
	2.80	2.80	−0.08	100.08	99.97
	4.51	4.52	−0.13	100.13	99.95
mean				100.013	100.063
variance				0.009	0.006
observations				3	3
F	1.48				
t value	0.72				
t critical[a]	2.78				
F critical[a]	19				

[a]F critical (19) and T critical two-tail (2.78). [b]Each result is the average of three separate determinations.

Table 4. Accurateness of the Estimated Differential Pulse Voltammetric Technique for Determination of TIR in Biological Fluids

	added (μg mL^{-1})	found (μg mL^{-1})	bias %[b]	recovery (%)	RSD[a] (%)
human urine 1	1.36	1.35	0.74	99.26	0.91
	3.7	3.72	−0.54	100.54	1.15
	5.68	5.69	−0.18	100.18	0.92
	7.1	7.11	−0.14	100.14	1.32
human serum	1.36	1.32	2.94	97.06	1.26
	3.7	3.65	1.35	98.65	1.05
	5.68	5.7	−0.35	100.35	0.84
	7.1	6.95	2.11	97.89	0.75

[a]RSD = relative standard deviation. [b]Mean of five measurements.

4. CONCLUSIONS

As a novel TIR sensor, the fabrication and the electrochemical characteristics of copper oxide nanoparticle-integrated carbon paste electrodes were described for sensitive and highly selective differential pulse voltammetric identification of TIR in pharmaceutical formulations and biological samples. Copper oxide as a proper electrode modifier exhibited an electrocatalytic activity toward the oxidation of TIR with a diffusion-controlled reaction accompanied by the involvement of one electron/proton as assumed by the scan rate studies, pH, and molecular orbital calculations. Enhanced performance was achieved in the TIR concentration ranging from 0.060 to 7.41 μg mL^{-1}. Based on the sensitivity and selectivity of the proposed CuONPs/CPE sensor, a sensitive and reliable voltammetric protocol was established for assaying of TIR in pharmaceutical dosage forms, plasma, and urine samples.

■ ASSOCIATED CONTENT

Supporting Information

The Supporting Information is available free of charge at https://pubs.acs.org/doi/10.1021/acsomega.2c07790.

Outlines of methodology of antioxidants and cytotoxicity and spectra recorded for the analysis (PDF)

https://doi.org/10.1021/acsomega.2c07790
ACS Omega 2023, 8, 5042−5049

AUTHOR INFORMATION

Corresponding Author

Nashwa M. El-Metwaly − *Department of Chemistry, Faculty of Science, Mansoura University, Mansoura 35516, Egypt;* orcid.org/0000-0002-0619-6206; Email: nmmohamed@uqu.edu.sa, n_elmetwaly00@yahoo.com

Authors

Ameena M. Al-bonayan − *Department of Chemistry, Faculty of Applied Sciences, Umm Al-Qura University, Makkah 21961, Saudi Arabia*

Jalal T. Althakafy − *Department of Chemistry, Faculty of Applied Sciences, Umm Al-Qura University, Makkah 21961, Saudi Arabia*

Ali Q. Alorabi − *Department of Chemistry, Faculty of Sciences, Albaha University, Albaha 65799, Saudi Arbia*

Nasser A. Alamrani − *Department of Chemistry, Faculty of Science, University of Tabuk, Tabuk 71474, Saudi Arabia*

Enas H. Aljuhani − *Department of Chemistry, Faculty of Applied Sciences, Umm Al-Qura University, Makkah 21961, Saudi Arabia*

Omaymah Alaysuy − *Department of Chemistry, Faculty of Science, University of Tabuk, Tabuk 71474, Saudi Arabia*

Salhah D. Al-Qahtani − *Department of Chemistry, College of Science, Princess Nourah bint Abdulrahman University, Riyadh 11671, Saudi Arabia*

Complete contact information is available at: https://pubs.acs.org/10.1021/acsomega.2c07790

Notes

The authors declare no competing financial interest.

Availability of data and materials: all data generated or analyzed during this study are included in this published article (and its Supporting Information files).

ACKNOWLEDGMENTS

The authors thank the Princess Nourah bint Abdulrahman University Researchers Supporting Project number (PNURSP2023R122) and Princess Nourah bint Abdulrahman University, Riyadh, Saudi Arabia.

REFERENCES

(1) Vickers, S.; Theoharides, A. D.; Arison, B.; Balani, S. K.; Cui, D.; Duncan, C. A.; Ellis, J. D.; Gorham, L. M.; Polsky, S. L.; Prueksaritanont, T.; Ramjit, H. G. In vitro and in vivo studies on the metabolism of tirofiban. *Drug Metabol. Dispos.* **1999**, *27*, 1360−1366.

(2) Ferrari, E.; Menabue, L.; Saladini, M. Characterization and metal affinity of Tirofiban, a pharmaceutical compound used in acute coronary syndromes. *BioMetals* **2004**, *17*, 145−155.

(3) McClellan, K. J.; Goa, K. L. Tirofiban. *Drugs* **1998**, *56*, 1067−1080.

(4) Oertel, R.; Köhler, A.; Koster, A.; Kirch, W. Determination of Tirofiban in human serum by liquid chromatography-tandem mass spectrometry. *J. Chromatogr., B* **2004**, *805*, 181−185.

(5) Jayakumar, B. Tirofiban Hydrochloride−Platelet GP IIb/IIIa Inhibitor. *Kerala Med. J.* **2010**, *3*, 25−27.

(6) Gong, J.; Shang, J.; Yu, H.; Wan, Q.; Su, D.; Sun, Z.; Liu, G. Tirofiban for acute ischemic stroke: systematic review and meta-analysis. *Eur. J. Clin. Pharmacol.* **2020**, *76*, 475−481.

(7) Akl, M. A.; Ahmed, M. A.; Ramadan, A. The Utility of HPLC-UV Cleaning Validation for the Determination of Tirofiban Residues. *J. Chromatogr. Sep. Tech.* **2013**, *4*, 1000178/1−1000178/5.

(8) Ranjitha, K. S.; Rao, A. L. Development and validation of new RP-HPLC method for the determination of Tirofiban in pharmaceutical formulation. *Int. J. Pharmaceut. Chem. Biol. Sci.* **2011**, *1*, 43−47.

(9) Serafimovska, M. D.; Janevik-Ivanovska, E.; Arsova-Sarafinovska, Z.; Djorgoski, I.; Ugresic, N. Development and validation of reverse phase high performance liquid chromatographic method for determination of tirofiban in serum. *Int. J. Pharm.* **2014**, *4*, 115−120.

(10) Darkovska-Serafimovska, M.; Janevik-Ivanovska, E.; Balkanov, T.; Ugresic, N. Development of alternative HPLC method for determination of tirofiban in rat serum. *Maced. J. Chem. Chem. Eng.* **2016**, *35*, 217−223.

(11) El-Bagary, R. I.; Elkady, I.; Farid, E. F.; Youssef, N. A.; Youssef, N. F. Stability study and validated reversed phase liquid chromatographic method for the determination of tirofiban hydrochloride in presence of tyrosine as a process impurity. *J. Chil. Chem. Soc.* **2018**, *63*, 3958−3967.

(12) Althakafy, J. T.; Kulsing, C.; Grace, M. R.; Marriott, P. J. Liquid chromatography - quadrupole Orbitrap mass spectrometry method for selected pharmaceuticals in water samples. *J. Chromatogr., A* **2017**, *1515*, 164−171.

(13) Althakafy, J. T.; Kulsing, C.; Grace, M. R.; Marriott, P. J. Determination of selected emerging contaminants in freshwater invertebrates using a universal extraction technique and liquid chromatography accurate mass spectrometry. *J. Separ. Sci.* **2018**, *41*, 3706−3715.

(14) Yin, Y. J.; Qiao, L.; Zhang, Q. M. HPLC determination of tirofiban using chiral mobile phase. *Chin. J. Pharm. Anal.* **2013**, *33*, 1012−1015.

(15) Huang, R.; Zhao, C.; Sun, J.; Wei, Q.*Determination of Tirofiban Hydrochloride/Sodium Chloride Injection by UV Spectrophotometry*; China Pharmacy, 1991, 05.

(16) El-Bagary, R. I.; Elkady, E. F.; Farid, N. A.; Youssef, N. F. Validated spectrofluorimetric methods for the determination of apixaban and tirofiban hydrochloride in pharmaceutical formulations. *Spectrochim. Acta, Part A* **2017**, *174*, 326−330.

(17) Hand, E. L.; Gilbert, J. D.; Yuan, A. S.; Olah, T. V.; Hichens, M. Determination of MK-383, a non-peptide fibrinogen receptor antagonist, in human plasma and urine by radioimmunoassay. *J. Pharmaceut. Biomed. Anal.* **1994**, *12*, 1047−1053.

(18) Siddiqui, M. R.; AlOthman, Z. A.; Rahman, N. Analytical techniques in pharmaceutical analysis: A review. *Arab. J. Chem.* **2017**, *10*, S1409−S1421.

(19) Ozkan, S. A.*Electroanalytical Methods in Pharmaceutical Analysis and Their Validation*; HNB Publishing, 2012.

(20) Ozkan, S. A.; Kauffmann, J. M.; Zuman, P.*Electroanalysis in Biomedical and Pharmaceutical Sciences: Voltammetry, Amperometry, Biosensors, Applications*; Springer, 2015.

(21) Ziyatdinova, G.; Budnikov, H. Electroanalysis of antioxidants in pharmaceutical dosage forms: state-of-the-art and perspectives. *Monatsh. Chem.* **2015**, *146*, 741−753.

(22) Althagafi, I. I.; Ahmed, S. A.; El-Said, W. A. Fabrication of gold/graphene nanostructures modified ITO electrode as highly sensitive electrochemical detection of Aflatoxin B1. *PLoS One* **2019**, *14*, No. e0210652.

(23) Shawky, A. M.; El-Tohamy, M. F. Highly functionalized modified metal oxides polymeric sensors for potentiometric determination of letrozole in commercial oral tablets and biosamples. *Polymers* **2021**, *13*, 1384.

(24) Elmosallamy, M. A.; Saber, A. L. Recognition and quantification of some monoamines neurotransmitters. *Electroanalysis* **2016**, *28*, 2500−2505.

(25) Kassem, M. A.; Hazazi, O. A.; Ohsaka, T.; Awad, M. I. Electroanalysis of pyridoxine at copper nanoparticles modified polycrystalline gold electrode. *Electroanalysis* **2016**, *28*, 539−545.

(26) Li, G.; Qi, X.; Wu, J.; Xu, L.; Wan, X.; Liu, Y.; Chen, Y.; Li, Q. Ultrasensitive, label-free voltammetric determination of norfloxacin based on molecularly imprinted polymers and Au nanoparticle-

functionalized black phosphorus nanosheet nanocomposite. *J. Hazard. Mater.* **2022**, *436*, 129107.
(27) Li, G.; Wu, J.; Qi, X.; Wan, X.; Liu, Y.; Chen, Y.; Xu, L. Molecularly imprinted polypyrrole film-coated poly(3,4-ethylenedioxythiophene):polystyrene sulfonate-functionalized black phosphorene for the selective and robust detection of norfloxacin. *Mater. Today Chem.* **2022**, *26*, 101043.
(28) Li, G.; Qi, X.; Zhang, G.; Wang, S.; Li, K.; Wu, J.; Wan, X.; Liu, Y.; Li, Q. Low-cost voltammetric sensors for robust determination of toxic Cd(II) and Pb(II) in environment and food based on shuttle-like α-Fe2O3 nanoparticles decorated β-Bi2O3 microspheres. *Microchem. J.* **2022**, *179*, 107515.
(29) Li, Q.; Wu, J. T.; Liu, Y.; Qi, X. M.; Jin, H. G.; Yang, C.; Liu, J.; Li, G. L.; He, Q. G. Recent advances in black phosphorus-based electrochemical sensors: A review. *Anal. Chim. Acta* **2021**, *1170*, 338480.
(30) Sannegowda, L. K.; Reddy, K. V.; Shivaprasad, K. H. Stable nano-sized copper and its oxide particles using cobalt tetraamino phthalocyanine as a stabilizer; application to electrochemical activity. *RSC Adv.* **2014**, *4*, 11367−11374.
(31) Al-Qahtani, S. D.; Hameed, A.; Alamrani, N. A.; Alharbi, A.; Shah, R.; Al-Ahmed, Z. A.; El-Metwaly, N. M. Zinc Oxide Nanostructured-Based Sensors for Anodic Stripping Voltammetric Determination of Darifenacin. *J. Electrochem. Soc.* **2022**, *169*, 066512.
(32) Liu, H.; Xiong, R.; Zhong, P.; Li, G.; Liu, J.; Wu, J.; Liu, Y.; He, Q. Nanohybrids of shuttle-like α-Fe2O3 nanoparticles and nitrogen-doped graphene for simultaneous voltammetric detection of dopamine and uric acid. *New J. Chem.* **2020**, *44*, 20797−20805.
(33) Li, Q.; Xia, Y.; Wan, X.; Yang, S.; Cai, Z.; Ye, Y.; Li, G. Morphology-dependent MnO2/nitrogen-doped graphene nanocomposites for simultaneous detection of trace dopamine and uric acid. *Mater. Sci. Eng., C* **2020**, *109*, 110615.
(34) Li, F.; Ni, B.; Zheng, Y.; Huang, Y.; Li, G. A simple and efficient voltammetric sensor for dopamine determination based on ZnO nanorods/electro-reduced graphene oxide composite. *Surface. Interfac.* **2021**, *26*, 101375.
(35) Li, G.; Zhong, P.; Ye, Y.; Wan, X.; Cai, Z.; Yang, S.; Xia, Y.; Li, Q.; Liu, J.; He, Q. A Highly Sensitive and Stable Dopamine Sensor Using Shuttle-Like α-Fe2O3 Nanoparticles/Electro-Reduced Graphene Oxide Composites. *J. Electrochem. Soc.* **2019**, *166*, B1552.
(36) Kokulnathan, T.; Wang, T. J.; Murugesan, T.; Anthuvan, A. J.; Kumar, R. R.; Ahmed, F.; Arshi, N. Structural growth of zinc oxide nanograins on carbon cloth as flexible electrochemical platform for hydroxychloroquine detection. *Chemosphere* **2023**, *312*, 137186.
(37) Ahmed, F.; Kokulnathan, T.; Umar, A.; Akbar, S.; Kumar, S.; Shaalan, N. M.; Arshi, N.; Alam, M. G.; Aljaafari, A.; Alshoaibi, A. Zinc Oxide/Phosphorus-Doped Carbon Nitride Composite as Potential Scaffold for Electrochemical Detection of Nitrofurantoin. *Biosensors* **2022**, *12*, 856.
(38) Kokulnathan, T.; Jothi, A. I.; Chen, S. M.; Almutairi, G.; Ahmed, F.; Arshi, N.; AlOtaibi, B. Integrating graphene oxide with magnesium oxide nanoparticles for electrochemical detection of nitrobenzene. *J. Environ. Chem. Eng.* **2021**, *9*, 106310.
(39) Kokulnathan, T.; Vishnuraj, R.; Wang, T. J.; Pullithadathil, B. Multidimensional nanoarchitectures of TiO2/Au nanofibers with O-doped C3N4 nanosheets for electrochemical detection of nitrofurazone. *Appl. Surf. Sci.* **2022**, *604*, 154474.
(40) Kokulnathan, T.; Wang, T. J.; Ahmed, F.; Alshahrani, T. Hydrothermal synthesis of ZnCr-LDH/tungsten carbide composite: a disposable electrochemical strip for mesalazine analysis. *Chem. Eng. J.* **2023**, *451*, 138884.
(41) Tajik, S.; Beitollahi, H.; Nejad, F. G.; Safaei, M.; Zhang, K.; Van Le, Q.; Varma, R. S.; Jang, H. W.; Shokouhimehr, M. Developments and applications of nanomaterial-based carbon paste electrodes. *RSC Adv.* **2020**, *10*, 21561−21581.
(42) Qian, L.; Durairaj, S.; Prins, S.; Chen, A. Nanomaterial-based electrochemical sensors and biosensors for the detection of pharmaceutical compounds. *Biosens. Bioelectron.* **2021**, *175*, 112836.
(43) Agnihotri, A. S.; Varghese, A.; M, M. Transition metal oxides in electrochemical and bio sensing: A state-of-art review. *Appl. Surf. Sci.* **2021**, *4*, 100072.
(44) Svancara, I.; Kalcher, K.; Walcarius, A.; Vytras, K.*Electroanalysis with Carbon Paste Electrodes*; CRC Press, 2019.
(45) Stanković, D.; Mehmeti, E.; Svorc, L.; Kalcher, K. New electrochemical method for the determination of β-carboline alkaloids, harmalol and harmine, in human urine samples and in Banisteriopsis caapi. *Microchem. J.* **2015**, *118*, 95−100.
(46) Zhang, Z.; Wang, E.*Electrochemical Principles and Methods*; Science Press: Beijing, 2000.
(47) Gosser, D. K.*Cyclic Voltammetry, Simulation and Analysis of Reaction Mechanisms*; Wiley VCH: New York, 1993.
(48) Elgrishi, N.; Rountree, K. J.; McCarthy, B. D.; Rountree, E. S.; Eisenhart, T. T.; Dempsey, J. L. A Practical Beginner's Guide to Cyclic Voltammetry. *J. Chem. Educ.* **2018**, *95*, 197−206.
(49) Laviron, E. Adsorption, autoinhibition and autocatalysis in polarography and in linear potential sweep voltammetry. *J. Electroanal. Chem.* **1974**, *52*, 355−393.
(50) Bard, A. J.; Faulkner, L. R.*Electrochemical Methods: Fundamentals and Applications*, 2nd ed.; Wiley: New York, 2004; p 594.
(51) Jouikov, V.; Simonet, J.Electrochemical reactions of sulfur organic compounds. *Encyclopedia of Electrochemistry*; Bard, A. J., Stratmann, M., Scholz, F.; etal, Eds.; Wiley-VCH Verlag GmbH & Co: Weinheim, Germany, 2007; Vol. *8*.
(52) Sitting, M.*Pharmaceutical Manufacturing Encyclopedia*, 3rd ed.; William Andrew Publishing: New York, 2007.

https://doi.org/10.1021/acsomega.2c07790
ACS Omega 2023, 8, 5042−5049